J. Materials, Conc. Struct., Pavements, JSCE, No. 613/V-42, 295-307, 1999 February

FRACTURE OF CONCRETE COVER - ITS EFFECT ON TENSION STIFFENING AND MODELING -

Hamed SALEM[1,2], Bernhard HAUKE[3] and Koichi MAEKAWA[4]

[1] Member of JSCE, Ph.D., Post Doctoral Fellow, Dept. of Civil Eng., The University of Tokyo (Hongo 7-3-1, Bunkyo-ku, Tokyo 113, Japan)
[2] Assistant Professor, Structural Engineering Department, Cairo University (Giza, Egypt)
[3] Member of JSCE, Ph.D., Dept. of Civil Eng., The University of Tokyo (Hongo 7-3-1, Bunkyo-ku, Tokyo 113, Japan)
[4] Member of JSCE, Dr. of Eng., Professor, Dept. of Civil Eng., The University of Tokyo (Hongo 7-3-1, Bunkyo-ku, Tokyo 113, Japan)

The aim of this study is to investigate the effect of non-sufficient concrete cover on the tension stiffness of reinforced concrete. Splitting cracks are predicted by simultaneously solving equilibrium among radial bond stresses, softening tensile stresses of splitting concrete planes and transverse stress on reinforcement. The bond behavior after splitting cracks is the point of study. The analytical model is derived from the micro-bond characteristics. An experimental program was carried out to verify the post-crack bond model proposed, and the analysis fairly agrees with the reality.

Key Words: *bond-slip-strain, tension stiffening, crack spacing, confining pressure, splitting crack, concrete cover*

1. INTRODUCTION

When concrete cover is not sufficient, longitudinal cracks, named as splitting cracks, are formed parallel to reinforcing bars. The occurrence of these cracks is a result of three dimensional bond transfer mechanisms. The deformed bars' lugs induce bearing stresses in surrounding concrete, resulting in conical compressive struts as shown in **Fig. 1**. The conical bond actions between bar and concrete can be resolved into radial and tangential components. Usually, the tangential one per unit area of reinforcing bar's surface is called bond stress, whereas the radial one is called confining stress. The radial stresses can be analogous to hydraulic pressure acting on a thick-walled concrete ring. When the tensile ring stresses, as illustrated in **Fig. 1**, exceed the cracking strength, the splitting crack is formed as shown in **Fig. 2**.

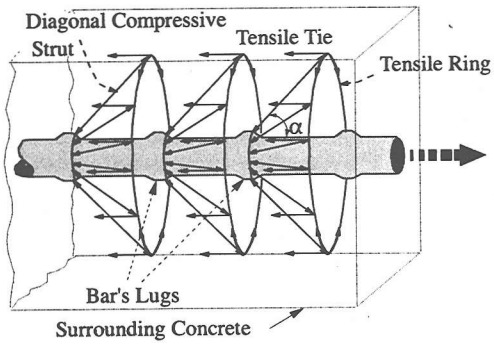

Fig. 1 Tensile ring force caused by diagonal bond struts

The bond behavior for concrete having such cracks was studied by Gambarova et al.[5]. Gambarova tested specimens with artificial splitting crack. By relating the splitting crack width with the confining pressure on the bars, an empirical formula was proposed for bond stresses after longitudinal splitting of concrete cover. Abrishami and Mitchell[10] studied the splitting cracks' effect on the tension stiffening of concrete. Specimens with shallow depth were targeted. Here the concrete cover was insufficient for both sides of the reinforcing bar concerned. The common members of civil structures are deep in general and the small cover of either side of the structural reinforcement does matter. Therefore, a less effect of splitting crack would exist. Salem and Maekawa[11), 12)] derived macroscopic tension stiffening from local bond stress development by assuming thick covers, which would lead to the full performance of bond stress formulated by Shima et al[4].

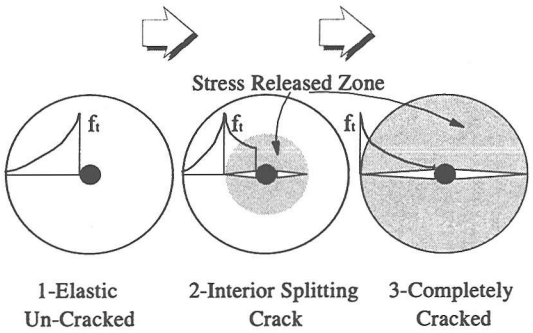

Fig. 2 Radial tensile stresses and splitting cracks

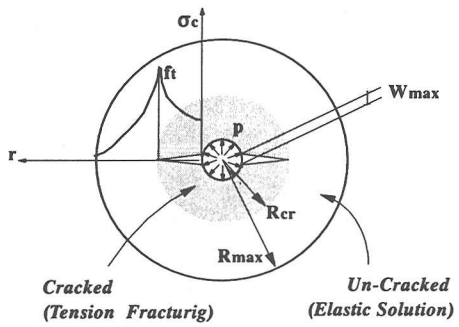

Fig. 3 Tangential stress developing in cracked and uncracked concrete

The aim of this study is to derive smeared model for reinforced concrete in tension from microscopic behavior, taking into account the possible reduction in bond stresses due to insufficient cover accompanying longitudinal splitting cracks. This study is the extension of authors' formulation on macro tension-stiffness[11), 12)] covering the case where pre-matured splitting crack is induced.

2. SPLITTING BOND STRESS

(1) Members without transverse reinforcement

The principal direction of bond force transferred between deformed reinforcing bars and surrounding concrete makes an angle with the bar axis. The bond forces can be resolved into radial and tangential components. Usually, the tangential one is called bond stress, whereas the radial one is called confining stress or pressure. The angle of inclination denoted by α (see **Fig. 1**) ranges from 45 to 80 degrees as reported by Goto[2)]. The radial stresses due to bond action act like hydraulic pressure acting on a thick-walled concrete ring. An elastic solution for the stresses in a thick-walled cylinder subjected to internal pressure is given by Timoshenko[1)], and Avalle et al.[9)] as,

$$\sigma_r = p\, R^2_{cr}\left(\frac{1-\frac{R^2_{max}}{r^2}}{R^2_{max}-R^2_{cr}}\right)$$

$$\sigma_t = p\, R^2_{cr}\left(\frac{1+\frac{R^2_{max}}{r^2}}{R^2_{max}-R^2_{cr}}\right) \qquad (1)$$

where, σ_r, σ_t: radial and tangential stresses at radial distance denotd by r from the centre of the bar, p: radial pressure, R_{cr}: radius of cracked concrete zone, R_{max}: cover of concrete + $\Phi/2$ and Φ: bar diameter.

These equations are valid for the uncracked concrete. However, in cracked concrete, the tension fracturing zone develops as illustrated in **Fig. 3**.

According to Avalle et al.[9)], the bond pressure which causes a splitting crack of radius R_{cr} can be computed by equilibrating the bond pressure p with the hoop tensile stresses in both the cracked and uncracked concrete as,

$$p = \frac{2f_t}{\Phi}\left(R_{cr}\left(\frac{R_{max}^2 - R_{cr}^2}{R_{max}^2 + R_{cr}^2}\right) + \int_{\Phi/2}^{Rcr}\left(\frac{\sigma_c(w(r))}{f_t}\right)dr\right) \qquad (2)$$

where, f_t is the tensile strength, w(r) is the splitting crack width at radius r and $\sigma_c(w(r))$ is the residual tensile stresses corresponding to crack width equal to w(r). The tension softening model adopted here is given by Uchida et al.[7)] as,

$$\sigma_c(w(r)) = f_t\left(1+0.5\left(\frac{f_t}{G_f}\right)w(r)\right)^{-3} \qquad (3)$$

where G_f is the fracture energy ranging from 0.1 to 0.15 N/mm for plain normal concrete [7)].

In Eq.(2) [illegible], Avalle assumed two propagating splitting cracks. This assumption agrees with the experimental observation of Morita and Kaku[3)] who reported that two or three splitting cracks propagate to surface of a concrete cylinder in pull-out tests. Moreover, in structural members, this is usually the case where splitting cracks propagate towards the

side of less cover. Avalle also assumed tangential strain compatibility by equating the circumferential elongation at the surface of reinforcing bar and at the crack propagation front with the concrete elasticity denoted by E_c as,

$$2\pi R_{cr}\frac{f_t}{E_c} = 2w_{max} + \left(2\pi\frac{\Phi}{2} - 2w_{max}\right)\frac{\sigma_c(w_{max})}{E_c} \qquad (4)$$

Using Eq. (4), the splitting crack width at the reinforcing bar's surface denoted by w_{max} is computed.

The crack width distribution has to be assumed in order to integrate the second part in the right hand term of Eq. (2). The authors assume the splitting crack width distribution to be linear, ranging from w_{max} at the surface of the reinforcement to zero at the crack front as follows.

$$w(r) = w_{max}\left(1 - \frac{r - \frac{\Phi}{2}}{R_{cr} - \frac{\Phi}{2}}\right) \qquad (5)$$

When the splitting cracks reach the surface of concrete, R_{cr} becomes equal to R_{max}. Thus, from Eq. (2) we have the ultimate pressure, p_{ult}, as,

$$p_{ult} = \frac{2}{\Phi}\int_{\phi/2}^{R_{max}} \sigma_c(w(r))dr \qquad (6)$$

By substituting Eq. (5) into Eq. (3) we have,

$$\sigma_c(w(r)) = f_t\left(1 + \frac{0.5 f_t\, w_{max}\left[R_{max} - r\right]}{G_f\left[R_{max} - \frac{\Phi}{2}\right]}\right)^{-3} \qquad (7)$$

Substitution of Eq. (7) into Eq. (6) yields,

$$p_{ult} = \frac{2f_t}{\Phi}\int_{\frac{\Phi}{2}}^{R_{max}}\left(1 + \frac{0.5 f_t\, w_{max}\left[R_{max} - r\right]}{G_f\left[R_{max} - \frac{\Phi}{2}\right]}\right)^{-3} dr \qquad (8)$$

Finally we have,

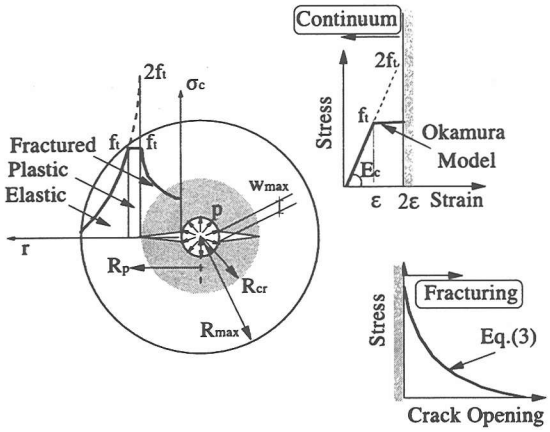

Fig. 4 Elasto-plastic and fracturing concrete in tension

$$p_{ult} = \left(\frac{a}{2b}\right)\left(1 - \frac{1}{\left(1 + bR_{max} - \frac{b\Phi}{2}\right)^2}\right) \qquad (9)$$

where,

$$a = \frac{2 f_t}{\Phi} \quad , \quad b = \frac{0.5 f_t\, w_{max}}{G_f\left(R_{max} - \frac{\Phi}{2}\right)} \qquad (10)$$

The previous equations assume that concrete is an elastic-damaging material in tension. But in reality, the rapid relaxation of tensile stress at the higher level is observed in concrete as a time dependency and plastic flow of deformation close to the cracking stresses may exist (Bujadham et al.[14]). Therefore, concrete plasticity is simply introduced with respect to a yielding plateau equal to double the cracking strain, as proposed by Okamura and Maekawa[6]. **Fig. 4** illustrates the idealized concrete plasticity in computing confining pressure.

The solution is derived by considering an exact elastic solution and determining the position with a tangential stress equal to f_t relative to the position with tangential stress equal to $2f_t$. At the location r = R_{cr}, the fictitious tangential stress equals to $2f_t$ and, for r = R_p, the substantial tangential stress must be the same as f_t. Then, by substituting these boundary conditions into Eq.(1), we have,

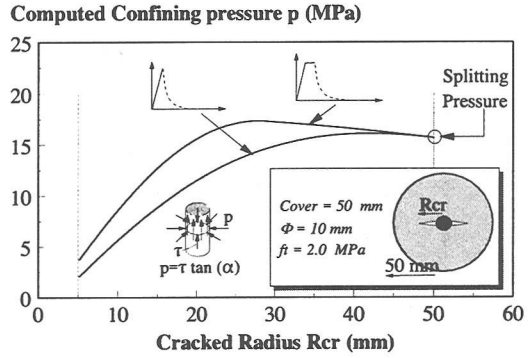

Fig. 5 Effect of concrete plasticity prior to cracking on splitting crack radius.

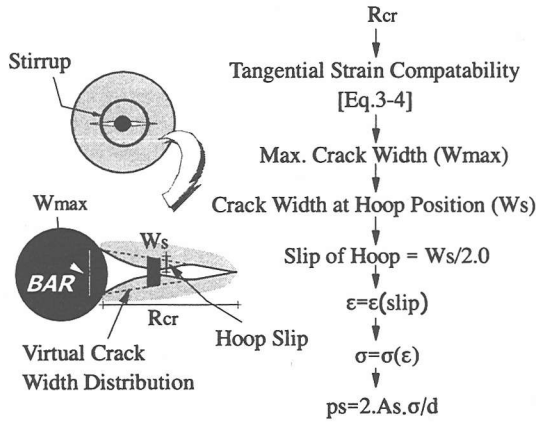

Fig. 6 Scheme of computing confining pressure due to hoop reinforcement

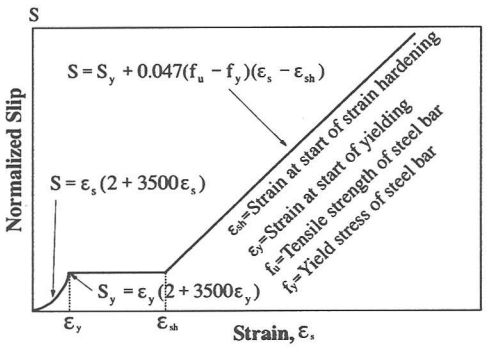

Fig. 7 Slip-strain relationship (Okamura and Maekawa[6])

$$2=\left(1+\frac{R_{max}^{\ 2}}{R_{cr}^{\ 2}}\right)\Bigg/\left(1+\frac{R_{max}^{\ 2}}{R_{p}^{\ 2}}\right) \tag{11}$$

$$R_p = R_{cr}\ R_{max}\sqrt{\frac{2}{R_{max}^{\ 2}-R_{cr}^{\ 2}}} \tag{12}$$

Consequently, the radial pressure p is computed as,

$$p=\frac{2f_t}{\Phi}\left(\begin{array}{l}(R_p-R_{cr})+R_p\left(\dfrac{R_{max}^{\ 2}-R_p^{\ 2}}{R_{max}^{\ 2}+R_p^{\ 2}}\right)\\ +\displaystyle\int_{\Phi/2}^{Rcr}\left(\frac{\sigma_c(w(r))}{f_t}\right)dr\end{array}\right) \tag{13}$$

The splitting pressure when concrete plasticity is considered is the same as the one when concrete plasticity is neglected. This is due to the fact that, the contribution of the uncracked concrete is zero, when the crack finally reaches the outer surface of concrete as shown in **Fig. 5**.

(2) Members with transverse reinforcement

If transverse reinforcement is arranged, the resistance to splitting cracks increases and the confining pressure on bars is accompanied. To consider the effect of hoops, the same analysis, adopted in the previous section, is used, and the confining stress produced by hoops is added (**Fig. 6**). The splitting crack distribution in this case will not be linear due to the existence of hoop reinforcement as shown in **Fig. 6**. Crack width vanishes at hoop location[8]. However, the real slip of hoop reinforcement, which equals to the deformations of the concrete adjacent to the hoop, can be obtained directly from the linear distribution. Geometrically the virtual splitting crack width at hoop position, computed from the linear distribution, is equal to twice the pull-out of hoops from concrete. For computing the strain of hoops at crack's location, the slip-strain relation, which was obtained by integrating the strain of steel based on the local bond-slip-strain model, was used (**Fig. 7**).

Hence, the confinement by the hoops can be coupled with fracturing of concrete. As can be seen from **Fig. 8**, before splitting crack tip reaches the concrete surface, the confining pressure gets higher whenever the hoop becomes closer to the bar. This is due to the fact that, the closer the hoop to the

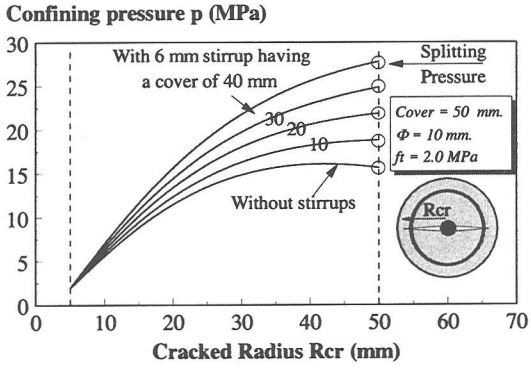

Fig. 8 Effect of hoops confining on splitting crack radius

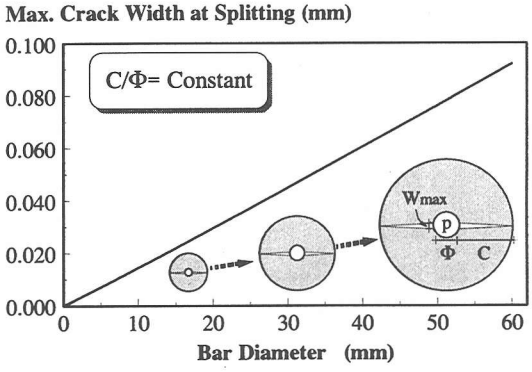

Fig. 9 Size effect on splitting crack width

bar, the higher the load required to cause the same crack width. The authors believe that, after the crack reaches the surface of concrete, different crack width distribution may exist with a wider crack opening at the concrete surface. Hence, the closer the hoop to the bar, the lower the confining stress.

3 . SIZE EFFECT SIMULATION

Many experimental works exhibit size effect that the nominal splitting stress decreases with the increase in the bar diameter[15]. The present model can successfully simulate the size effect of splitting pressure. Since the splitting crack width is proportional to the bar diameter as shown in **Fig. 9**, tension softening and hence splitting pressure of large-scale specimens is reduced. **Fig. 10** shows the computed size effect on splitting for geometrically similar specimens.

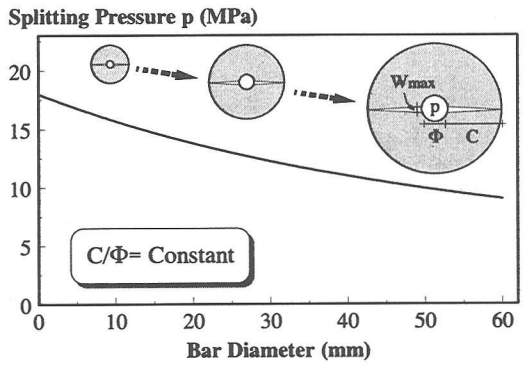

Fig. 10 Size effect on splitting pressure

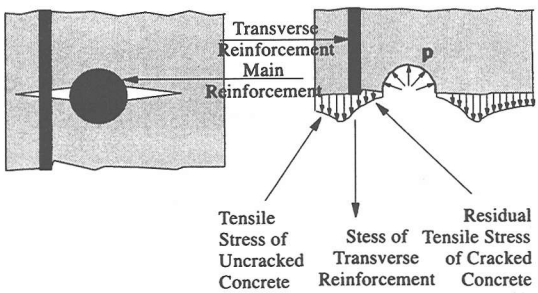

Fig. 11 Confining pressure acting on reinforcement

4 . BOND BEHAVIOR AFTER SPLITTING CRACKS OCCURENCE

After splitting cracks occur, the bond stress tends to be sensitively influenced by the reinforcement confinement. This confining action could be provided by the residual stresses transmitted between the faces of the split concrete and by hoop transverse reinforcement distributed along the main bar as illustrated in **Fig. 11**.

If the confining agent is not adequately placed around bars, splitting cracks develop abruptly along the re-bar and a sudden splitting failure may occur. On the other hand, when an adequate confining action is passively induced by the fracture of concrete cover, bond stress may increase up to pull-out failure or rupture of re-bar as illustrated in **Fig. 12**. However, the pull-out failure is practically not possible. This kind of failure is possible only when the bonded length is very short like some experimental simulations of bond mechanisms in which only one or few lugs are bonded.

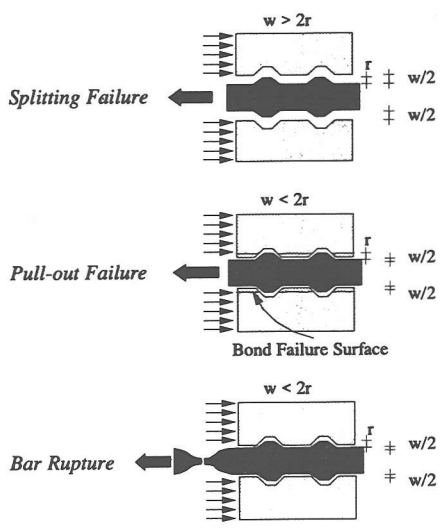

Fig. 12 Possible kinds of failure of reinforcing bars in tension

Gambarova et al.[5] developed an empirical formula for bond stress after formation of splitting cracks. The model represents the bond stress as a function of splitting crack width, w_{max}, and bar confining denoted by p as,

$$\tau = f_c'\left(0.042 - 0.288\left(w_{max}/\Phi\right)\right) + \left(\frac{0.258}{\left(\left(w_{max}/\Phi\right)+0.11\right)} - 1.018\right)p \qquad (14)$$

where f_c' is the compressive strength of concrete.

The bond-slip-strain model of Shima et al.[4], which is used in the analysis, does not take into account the effect of splitting cracks. In fact, the experiments on which the model is based were conducted by avoiding splitting failure with thick concrete cover. Thus, the model of Shima is simply modified in this study by changing the intrinsic slip function as follows.

$$\tau(\varepsilon, s) = \tau_0(s)\left(\frac{1}{1+10^5\varepsilon}\right) \qquad (15)$$

$$\tau_0(s) = f_c'\, k\,[\ln(1+5S)]^c \quad \text{before splitting (\textit{original form})} \qquad (16)$$

$$\tau_0(s) = \tau_1 \quad \text{after splitting}$$

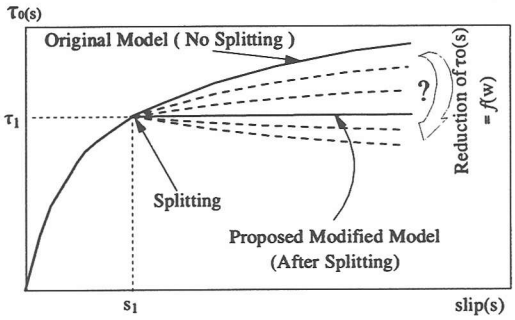

Fig. 13 Extension of Shima model[4]

where, S is non-dimensional slip=1000 s/Φ, s is slip, Φ is bar diameter , k is constant = 0.73, c is constant = 3 and $\tau_1 = \tau_0(S=S_1)$ where S_1 is non-dimensional slip at splitting.

The slip function after splitting might be higher or lower than the assumed one depending on the splitting crack width. The authors decided to tentatively assume plastic behavior of slip function after splitting. This simplified model is then discussed by comparing the analytical and the experimental macroscopic behavior of reinforced concrete later.

When the bond stress computed from Gambarova's model exceeds the original Shima's model, in case of very small crack width, the original model of Shima is used. This is due to the fact that, the bond stresses after splitting will not be higher than bond stresses before spitting.

5. ANALYSIS ALONG AXIS OF REINFORCEMENT

Based on the microscopic bond behavior, Salem and Maekawa[11),12)] computationally derived the macroscopic behavior of reinforced concrete in tension as illustrated in **Fig. 14**. In the analysis, local stresses of both concrete and reinforcement are evaluated. Hence, the average strains and stresses are computed over the whole range of analysis domain.

When the concrete cover is not sufficient, splitting of concrete cover may occur and the possible reduction of bond stresses has to be checked. Here, both Gambarova's model and Shima's modified model are used with coupling as explained in the previous section. As illustrated in **Fig. 14**, five governing equations are simultaneously solved after formation of splitting cracks. One more unknown (splitting crack width, w) is accompanied with the additional equation (Eq.(14)).

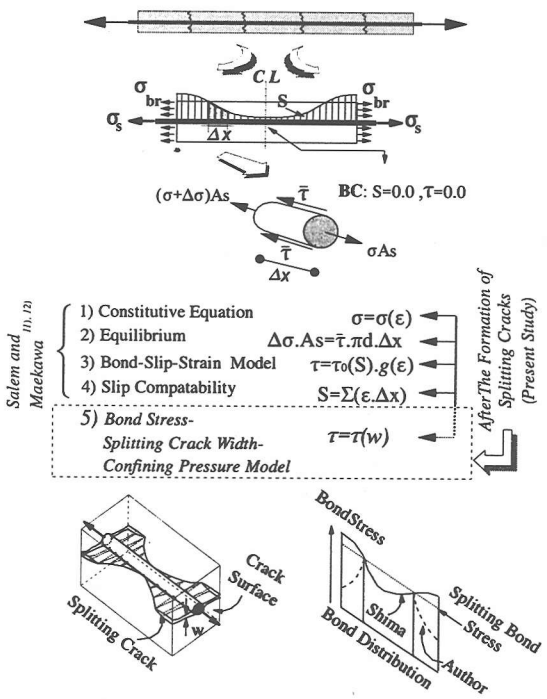

Fig.14 Scheme of solving bond governing equations with finite discretization

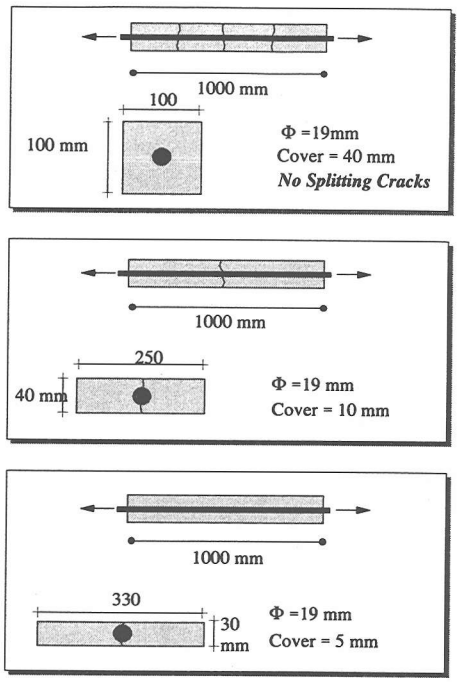

Fig.16 Case study for cover effect on tension stiffness

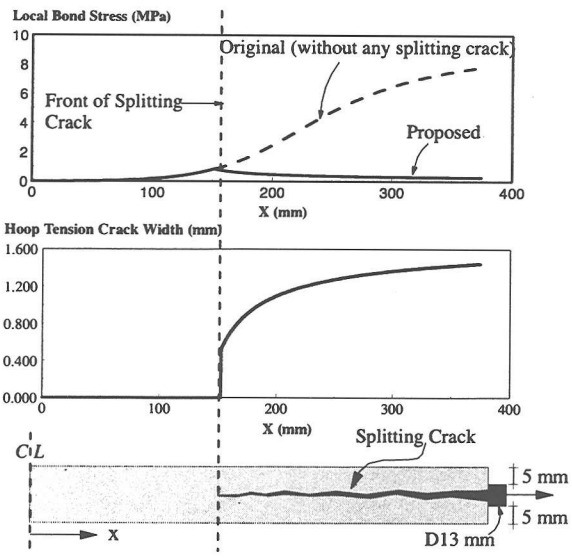

Fig.15 Analytical sample for splitting crack width and reduction of bond stresses

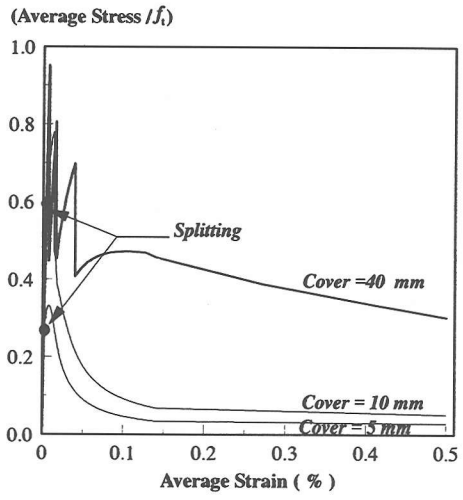

Fig.17 Case study for cover effect on the tension stiffening: analytical results

Fig.15 illustrates a sample of computations, in which the splitting crack width and the bond stress are plotted along a bar of 13 mm diameter, 750 mm long, and concrete cover is 5 mm on either sides. The hoop tension crack width increases close to the transverse cracks, where the bond stresses are significantly decreased.

Fig. 16 illustrates the analysis of three members having the same reinforcement ratio but with different geometry and cover thickness. Cross-sections of 100 × 100 mm, 40 × 250 mm and 30 × 330 mm are used. The corresponding concrete covers are 40, 10 and 5 mm, respectively. No hoop reinforcement is placed in analysis. For the 40 mm-cover specimen, the model predicts no splitting crack and three transverse cracks over the total length of 1000 mm. For the 10 mm-cover specimen, analysis predicts splitting cracks with only one transverse crack, while for the 5 mm-cover specimen no transverse crack is expected and longitudinal cracks are predicted in analysis. The tension stiffening is affected by the longitudinal cracks and the corresponding reduction of bond stresses. The smaller the cover-concrete, the larger the reductions in tension stiffening of concrete as shown in **Fig. 17**.

6. EXPERIMENTAL VERIFICATION

(1) Abrishami and Mitchell's Experiments[10]

For experimental verification, specimens tested by Abrishami and Mitchell[10] were analyzed. Abrishami tested five tension specimens. All of the specimens had a length of 1500 mm. A single reinforcing bar, with a minimum concrete cover on two faces of each specimen of 40 mm, was provided. Reinforcement ratio of 1.23 percent was used in all specimens. Reinforcing bars of diameters 11.3, 16, 19.5, 25.2 and 29.9 mm were used, respectively. **Fig. 18** through **Fig. 22** show a comparison between the authors' analysis and the experiment. These figures show both member behavior and the tension stiffening of concrete. It should be mentioned that the experimental tension stiffening could be computed only before yielding of reinforcing bars, since the steel is in the elastic range and the concrete contribution of carrying load can be computed by subtracting the reinforcement contribution as follows.

$$\bar{\sigma}_c = \bar{\sigma}_t - \rho(\bar{\varepsilon} E_s)$$

$$\bar{\sigma}_t = \frac{T}{A_g} \qquad (17)$$

$$\bar{\varepsilon} = \frac{\Delta l}{l}$$

where, T is the tensile load, A_g is the cross sectional area, Δl is the elongation and l is the total length of the specimen. It has also to be mentioned that, the initial drying shrinkage of the specimens is not considered in the author's analysis. The analytical results show a fair agreement with the experiment.

(2) Authors' Experiments

For experimental verification, two specimens of two meters length were tested. The specimens details are shown in **Fig. 23**. Each specimen is reinforced with two 10 mm deformed bars. A twenty mm-thick steel plate is punched as shown in **Fig. 23** and **Fig. 24**, and the main reinforcement is attached to the plate by means of nuts. A PC tendon is attached at the center of the plate by a nut as shown in **Fig. 23** and **Fig. 24**. The testing machine load is applied directly to this tendon. The specimen elongation was measured by a box-type displacement transducers which is fixed to the steel plate as illustrated in **Fig. 23.**

The specimens cross sections, reinforcement and concrete cover are identical. But, one of them has no hoops, while the other is transversely reinforced with 6 mm hoops (**Fig. 23** and **Fig. 25**). The ratio of cover to bar diameter in both specimens is 1.0, which would give no tension stiffening and no transverse cracks according to Abrishami and Mitchell[10]. The authors deemed that Abrishami's model might be valid primarily for the cases of shallow depth and insufficient cover from both sides. The tested specimens in this study represent the more common case of large sized reinforced concrete. The behavior is expected to be deviant from Abrishami's model since different confining and bond properties are expected.

Fig 26 through **Fig 29** illustrate the analytical and experimental results. **Fig. 26** and **Fig. 28** show the load-elongation relationship, while **Fig. 27** and **Fig. 29** show the tension stiffening of concrete in comparison with Abrishami's model. From those figures, it can be concluded that the author prediction is fairly in agreement with the experiment and that Abrishami's model underestimates the tension stiffening.

The analysis presents splitting load of 49 kN in specimen (1) and no splitting in specimen (2). The observed splitting load of specimen (1) was 45 kN with a deviation of 8%, while no splitting crack was observed in specimen (2) reinforced with transverse reinforcement as shown in **Fig. 30**. Also, the predicted crack spacing was close to the experiment with deviation of 12% and 19%, respectively.

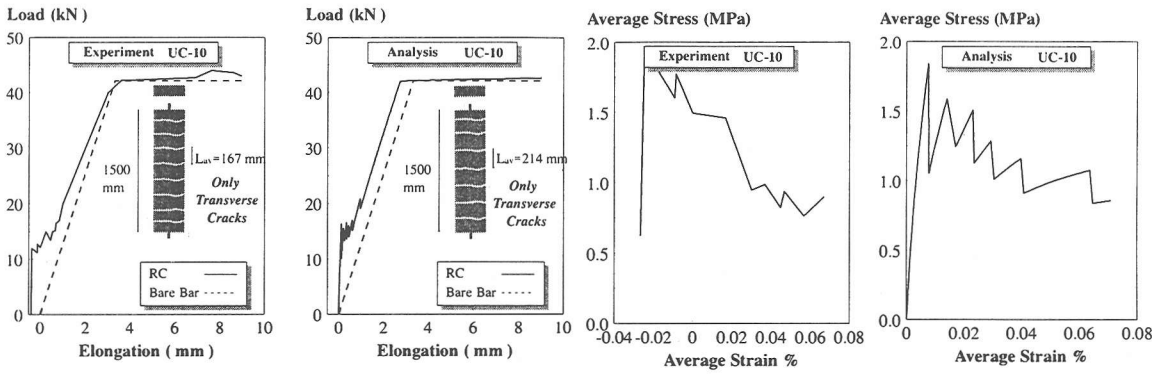

a) Member Response

b) Tension Stiffening of Concrete

Fig.18 Comparison between authors' analysis and experimental work of Abrishami and Mitchell[10]: (Specimen UC-10)

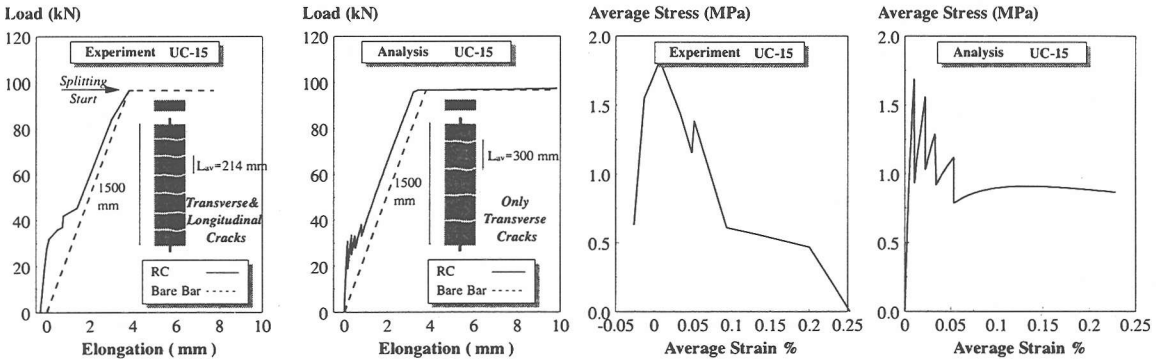

a) Member Response

b) Tension Stiffening of Concrete

Fig.19 Comparison between authors' analysis and experimental work of Abrishami and Mitchell[10]: (Specimen UC-15)

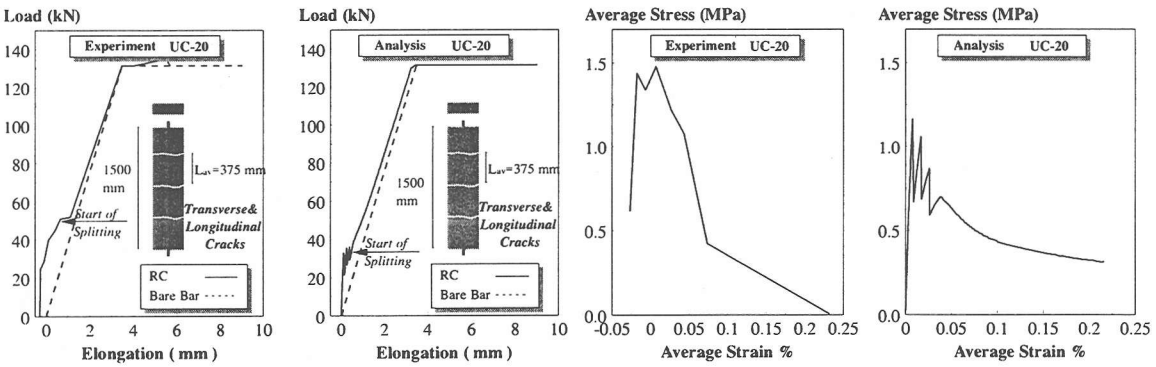

a) Member Response

b) Tension Stiffening of Concrete

Fig.20 Comparison between authors' analysis and experimental work of Abrishami and Mitchell[10]: (Specimen UC-20)

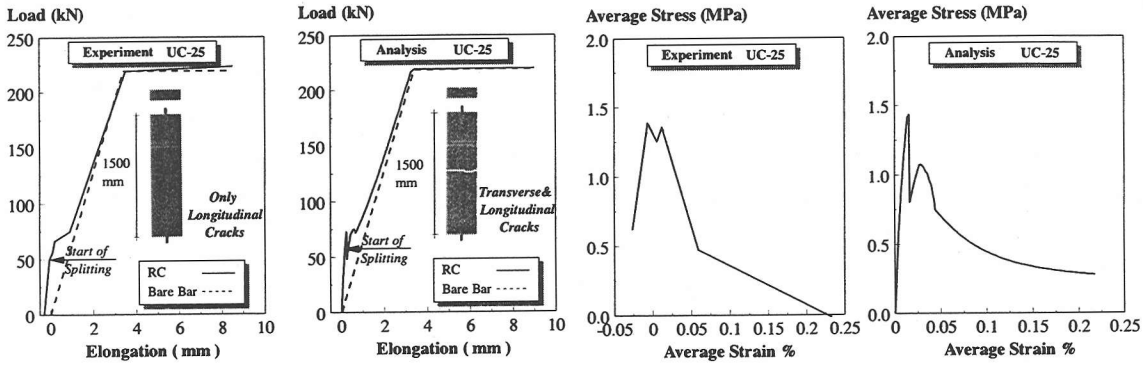

a) Member Response

b) Tension Stiffening of Concrete

Fig.21 Comparison between authors' analysis and experimental work of Abrishami and Mitchell[10]: (Specimen UC-25)

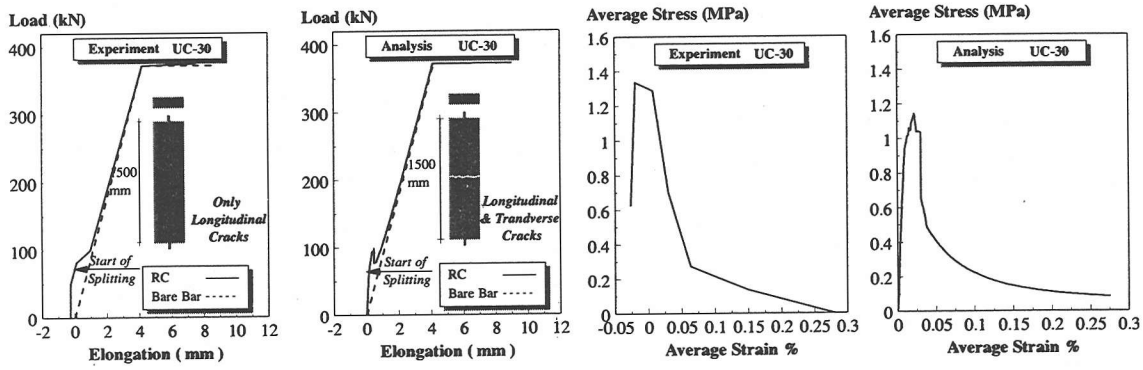

a) Member Response

b) Tension Stiffening of Concrete

Fig.22 Comparison between authors' analysis and experimental work of Abrishami and Mitchell[10]: (Specimen UC-30)

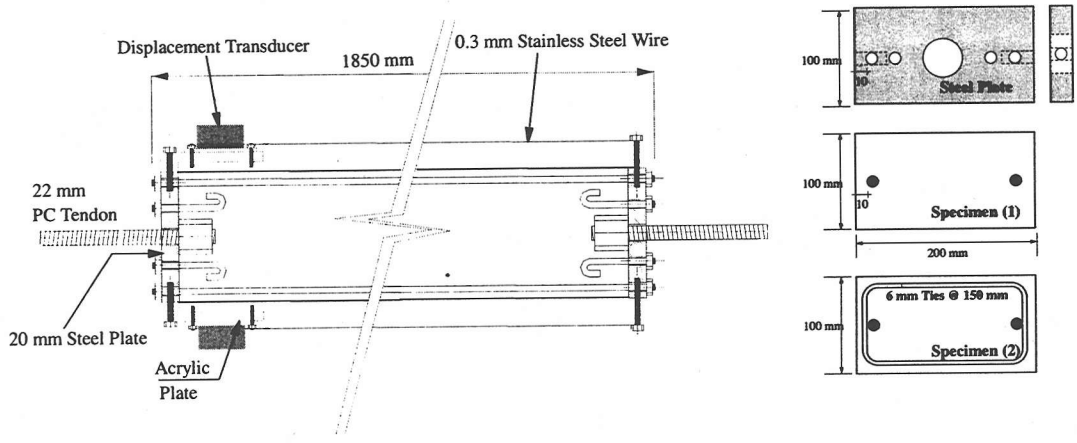

Fig. 23 Details of test specimens

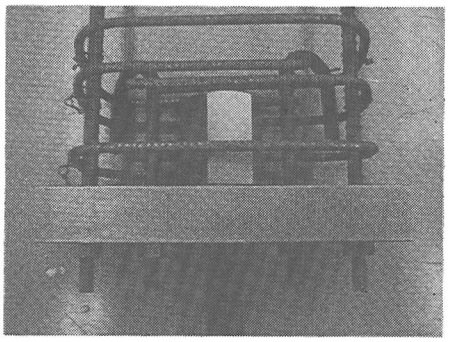

Fig. 24 PC tendon connection to the specimen

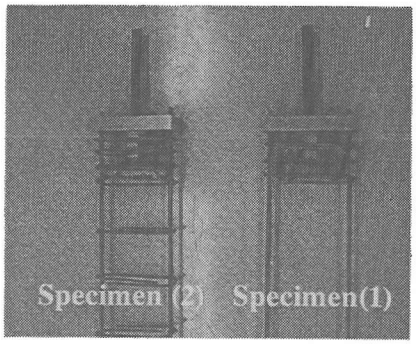

Fig. 25 Reinforcement details of test specimens

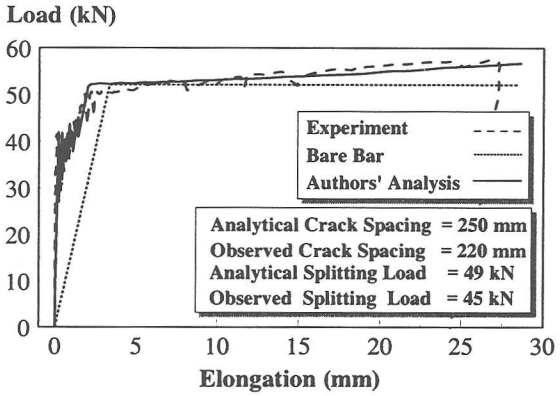

Fig. 26 Results of specimen (1): load-elongation relationship

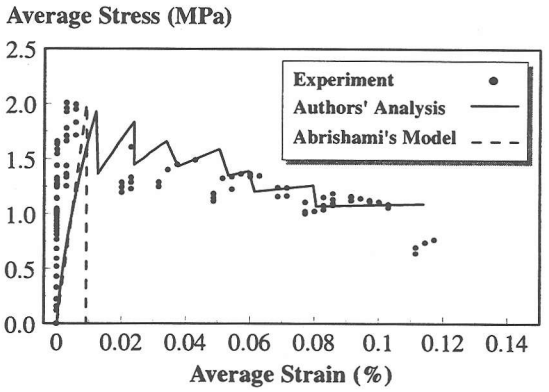

Fig. 27 Results of specimen (1): tension stiffening of concrete (before yielding)

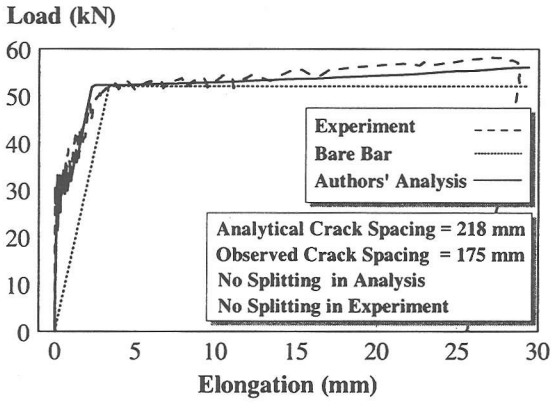

Fig. 28 Results of specimen (2): load-elongation relationship

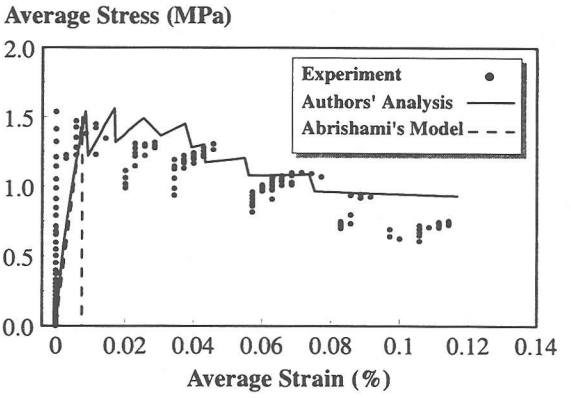

Fig. 29 Results of specimen (2): tension stiffening of concrete (before yielding)

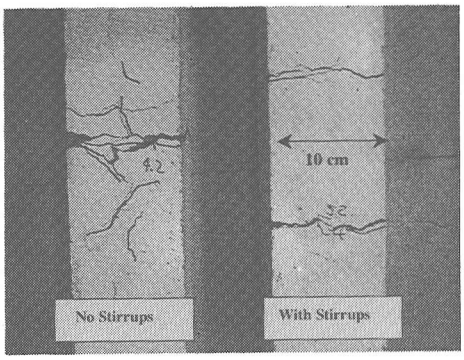

Fig. 30 Observed crack pattern of test specimens

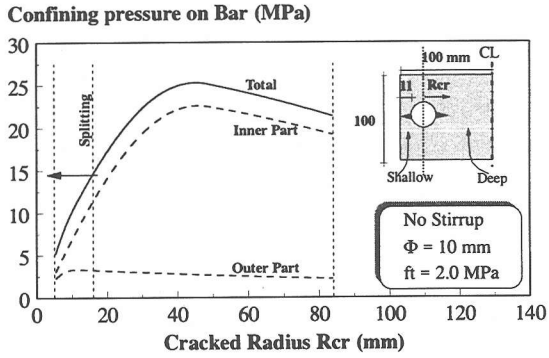

Fig. 31 Confining of bars of specimen (1)

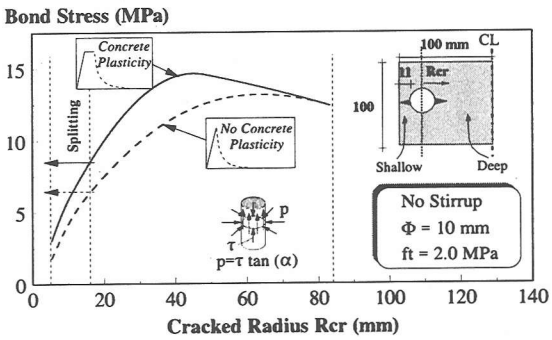

Fig. 32 Concrete plasticity effect on confining and bond of bars of specimen (1)

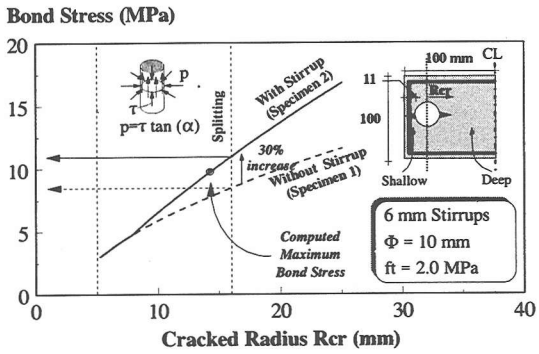

Fig. 33 Bond Stresses of bars of specimen (2)

In the analysis of the two specimens, the bond stresses were not affected by splitting cracks. In fact, the original bond model of Shima was used, since Gambarova's model gave bond stresses higher than Shima's model due to the huge confinement of bars even after splitting cracks' occurrence. **Fig. 31** illustrates the confining pressure on bars of specimen (1). If we consider the bar cross section divides the concrete into two zones, one is in the shallow side while the other is in the deep side, it can be seen that, the confinement of the deep side of concrete is the predominant one. In Abrishami's experiment, this confining action developing inside the specimen does not exist, leading to the great reduction of bond stresses.

Fig. 32 illustrates the computed bond stress of bars of specimen (1) as a function of the cracked radius, with and without taking the concrete plasticity in tension into consideration. As can be seen from this figure, the effect of concrete plasticity cannot be neglected. If it is neglected, the computed splitting bond stress would be 6.3 MPa instead of 8.4 MPa and the computed splitting load would be 32 kN instead of 49 kN, which is far from the experiment observations.

Fig. 33 illustrates the computed bond stress on bars of specimen (2) in a comparison to that of specimen (1). Due to the confinement action of steel tie in specimen (2), a 30% increase in bond stress required to cause splitting of cover is computed. The computed maximum local bond stress in this specimen did not reach the splitting bond stress as shown in **Fig. 33**. Based on this, the splitting load increased and no longitudinal cracks were expected. This agrees well with the experimental observations.

7. CONCLUSIONS

Based upon the tension softening of plain concrete, the radial bond stresses, and hence the splitting load of tension members with non-sufficient cover can be predicted.

The effect of splitting cracks on the bond properties, and tension stiffening is discussed. The

possible reduction in tension stiffening due to longitudinal cracks can be predicted

The effect of splitting cracks on the bond properties, and tension stiffening is huge for structural members with shallow thickness, like thin shells, where the concrete cover is not sufficient from all sides. However, this effect is negligible for deep structural members, like beams, even if the concrete cover is not sufficient. This is due to the effect of confinement action of the deep side of concrete.

REFERENCES

1) Timoshenko, S.: *Strength of Materials. Part II: Advanced Theory and Problems*, Princeton, N. J., D. Van Nostrand Company Inc., pp. 205-210, 1956.
2) Goto, Y.: Cracks formed in concrete around deformed tension bars, *ACI Journal*, Proceedings Vol. 68, No. 4, pp. 244-251, 1971.
3) Morita, S. and Kaku, T.: Splitting bond failure of large deformed reinforcing bars, *ACI Journal*, Proceedings Vol. 76, pp. 93-110, 1979.
4) Shima, H., Chou, L., and Okamura, H.: Micro and macro models for bond in reinforced concrete, *Journal of The Faculty of Engineering*, The University of Tokyo (B), Vol. 39, No 2, 1987.
5) Gambarova, P., Rosati, G., and Zasso, B.: Steel-to-concrete bond after concrete splitting: constitutive laws and interface deterioration, *Materials and Structures*, Vol. 22, pp. 347-356, 1989.
6) Okamura, H. and Maekawa, K.: *Nonlinear Analysis and Constitutive Models of Reinforced Concrete*, Gihodo, Tokyo, 1991.
7) Uchida, Y., Rokugo, K. and Koyanagi, W.: Determination of tension softening diagrams of concrete by means of bending tests, *Proc. of JSCE*, Vol. 14, No. 426, pp. 203-212, 1991.
8) Maekawa, K. and Qureshi, J.: Stress transfer across interfaces in reinforced concrete due to aggregate interlock and dowel action, *Journal of Materials, Concrete Structures and Pavements, JSCE*, Vol.34, No. 557, pp 159-172, 1997.
9) Avalle, M., Iori, I. and Vallini, P.: Analisi numerica del comportamento di elementi in conglomerato armato semplicemente tesi, *Studi E Ricerche*, Vol. 14, pp. 29-54, 1993. (*In Italian*)
10) Abrishami, H. and Mitchell, D.: Influence of splitting cracks on tension stiffening, *ACI Structural Journal*, Vol.93, No.6, pp. 703-710, 1996.
11) Salem, H. and Maekawa, K.: Tension stiffness for cracked reinforced concrete derived from micro-bond characteristics, *Proc. of JCI*, Vol.19, No.2, pp. 549-554, 1997.
12) Salem, H. and Maekawa, K.: Computational model for tension stiffness of cracked reinforced concrete derived from micro-bond characteristics, *Proc. Of the Sixth East Asia-Pacific Conference on Structural Engineering & Construction*, Taipei, Vol.3, pp. 1929-1934, 1998.
13) Salem, H., Hauke, B. and Maekawa, K.: Concrete cover effect on tension stiffness of cracked reinforced concrete, *Proc. of JCI*, Vol. 20, No.3, pp. 97-102, 1998.
14) Bujadham, B., Harada, S. and Maekawa, K.: Temperature and tensile stress path dependent models for tensile strength of concrete, *Proc. of JCI*, Vol.10, No.3, pp. 721-726, 1988.
15) Saitoh, S., Yoshii, Y. and Iizima, M.: Anchorage capacity of ribbed steel pipes embedded in concrete, *Proc. of JSCE Annual Convention*, Vol.50, pp. 800-801, 1995.

(Received June 2, 1998)

かぶりコンクリートの破壊を考慮した鉄筋コンクリートの引張剛性モデル

サレム ハメッド・ハウケ ベルンハルド・前川宏一

本研究の目的は，かぶりコンクリートの付着ひび割れ以後の，鉄筋コンクリートの引張剛性を与える構成モデルについて，論じたものである．付着割裂ひび割れは，鉄筋軸方向の付着応力，鉄筋周方向の引張軟化応力，および鉄筋自体の応力に関する釣り合いを解くことによって求められることを示した．割裂ひび割れを生じた後は，鉄筋周方向の変形適合条件と軸方向の付着残存応力を与えることで算定する方法を提示した．提案したひび割れ発生後の付着モデルの妥当性を検証するために，かぶりの薄い試験体を用いた実験を行い，解析結果が実際の挙動を模擬できることを確認した．